Chemical Physics Letters 471 (2009) 85–91

Contents lists available at ScienceDirect

Chemical Physics Letters

journal homepage: www.elsevier.com/locate/cplett

Broadband dielectric response of dichloromethane

Johannes Hunger [a], Alexander Stoppa [a], Andreas Thoman [b], Markus Walther [b], Richard Buchner [a,*]

[a] Institut für Physikalische und Theoretische Chemie, Universität Regensburg, D-93040 Regensburg, Germany
[b] Department of Molecular and Optical Physics, Albert-Ludwigs-Universität Freiburg, D-79104 Freiburg, Germany

ARTICLE INFO

Article history:
Received 17 December 2008
In final form 10 February 2009
Available online 13 February 2009

ABSTRACT

A systematic study of the dielectric response of dichloromethane over a broad frequency range ($8.5 \leqslant \nu/\mathrm{GHz} \leqslant 1000$; $\leqslant 4.3$ THz at 25 °C) at temperatures from 5 to 35 °C is reported. The spectra are best described by a superposition of three contributions. The dominating loss peak at ~70 GHz, fitted by a modified Debye equation accounting for inertial rise, represents the rotational diffusion of molecular dipoles. Additionally, two libration modes contribute, which are described by damped harmonic oscillators of resonance frequencies ~0.9 THz and ~2.1 THz. While the latter modes reflect the anisotropy of the dichloromethane molecule, the diffusive reorientation at long times appears to be rather isotropic.

1. Introduction

Due to its low boiling point (40 °C [1]), high density (1.3266 kg dm^{-3} [1]) and its immiscibility with hydrogen-bonding solvents like water, dichloromethane (DCM, CH_2Cl_2, Fig. 1) is widely used as a solvent in synthetic chemistry and technical applications, especially for separation processes [2]. Being a small molecule with the same C_{2v} symmetry and similar gas-phase dipole moment as water (DCM: $\mu = 1.61$ D [3]; H_2O: 1.85 D [1]) but without the ability to form H-bonds, the structure and dynamics of liquid DCM received considerable attention in the 1980s, when it was selected by the European Molecular Liquids Group as one of the target compounds for a collaborative project on the consistent evaluation of molecular dynamics in liquids [4].

At that time the far-infrared absorption spectrum of pure DCM [5,6] and its mixtures [3] were studied in some detail in the 30—200 cm^{-1} region, albeit with the limited accuracy then accessible. The aim was to gain information on intermolecular vibration and libration motions and to test interaction potentials for computer simulations [7]. However, only a small number of studies [8–10] explored the adjoining microwave to mm-wave frequencies because this region at ~70 GHz, where the main dielectric dispersion occurs [8], was and to some extent still remains difficult to access. To our knowledge the present investigation is the first study that addresses the temperature dependence of the dielectric spectrum of DCM in the GHz to THz region.

Due to its sensitivity to all kinds of dipole fluctuations dielectric spectroscopy (DS) is an efficient tool to study the dynamics and interaction in liquids [11,12]. Like conventional (far-)infrared spectroscopy DS probes the total polarization, $\vec{P}(t)$, of a sample in a time-dependent field, $\vec{E}(t)$, albeit at lower frequencies and thus longer timescales. In DS this response is conventionally expressed in terms of the complex permittivity spectrum, $\hat{\varepsilon}(\nu) = \varepsilon'(\nu) - i\varepsilon''(\nu)$. The relative permittivity $\varepsilon'(\nu)$ shows a dispersion from the static permittivity, ε, to the high-frequency limit ε_∞. The dielectric loss, $\varepsilon''(\nu)$, expresses the energy dissipation which arises from the coupling of $\vec{E}(t)$ to dipole fluctuations.

In this Letter, we report the dielectric spectra of DCM in the temperature range of 5–35 °C, covering the frequency range of $8.5 \leqslant \nu/\mathrm{GHz} \leqslant 1000$ (0.28—33cm^{-1}). At 25 °C the spectrum was extended up to ~4.3 THz (144 cm^{-1}) by including literature data [5]. A thorough investigation of DCM dynamics appears to be timely because in contrast to previous assumptions [7] recent simulations and cluster calculations showed the importance of the quadrupole moment for the interactions in liquid DCM [13] and indicated a strong contribution of induced dipoles to the far-infrared spectrum [14]. Additionally, existing information on the dynamics of DCM obtained with dielectric/far-infrared [5,6], NMR [15], and Raman [16] spectroscopies is somewhat conflicting. As will be shown below the present data resolve most of these discrepancies and should thus help to improve the existing potential models. Last but not least the proper characterization of $\hat{\varepsilon}(\nu)$ for pure DCM is worthwhile because DCM solutions receive increasing attention in dielectric studies [17–20] and DCM appears to be a suitable standard for the calibration of certain dielectric spectrometers [21].

2. Experimental

Dichloromethane was obtained from Acros Organics, Belgium (analytical grade, >99.99%) and stored over freshly activated molecular sieve (3 Å). Coulometric Karl–Fischer titration yielded a water content of <5 ppm for the investigated sample. Although

* Corresponding author. Fax: +49 941 943 4532.
E-mail address: Richard.Buchner@chemie.uni-regensburg.de (R. Buchner).

0009-2614/$ - see front matter © 2009 Elsevier B.V. All rights reserved.
doi:10.1016/j.cplett.2009.02.024

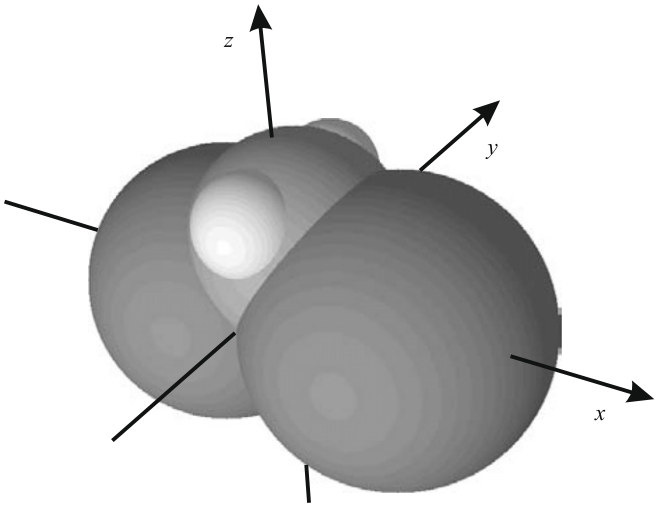

Fig. 1. Dichloromethane with its axes of inertia. Moments of inertia for rotation around x, y and z are $I_x = 2.62 \times 10^{-47}$ kg m^2, $I_y = 25.26 \times 10^{-47}$ kg m^2, and $I_z = 27.37 \times 10^{-47}$ kg m^2 [8]. The dipole moment of magnitude $\mu = 1.61$ D [3] is parallel to the z-axis.

the concentration of 1-pentene, added as a stabilizer to DCM by the manufacturer, was below the detection limit samples were kept at 35 °C for at least 3 h prior to measurements to avoid evaporation of the stabilizer during data collection.

Complex permittivity spectra, $\hat{\varepsilon}(\nu)$, were determined in the frequency range of $8.5 \leqslant \nu/\mathrm{GHz} \leqslant 1000$ by combining data obtained with four waveguide interferometers (IFM) [22] at $8.5 \leqslant \nu/\mathrm{GHz} \leqslant 89$ and a transmission THz-time-domain spectrometer (THz-TDS) [23] covering $0.117 \leqslant \nu/\mathrm{THz} \lesssim 1.0$. Except for the X-band IFM (8.5–12 GHz), operating only in the temperature range of $15 \leqslant \vartheta/^\circ\mathrm{C} \leqslant 35$, all instruments cover $5 \leqslant \vartheta/^\circ\mathrm{C} \leqslant 35$ with an accuracy of ±0.05 °C for the IFM and ±1 °C for the THz-TDS. None of these instruments requires calibration with a dielectric standard. As can be seen from Fig. 2 there is a seamless fit of the data points obtained with the various instruments, indicating the absence of systematic errors in $\hat{\varepsilon}(\nu)$.

At 25 °C the frequency range could be extended to 2 THz with a THz-TDS in reflection geometry [24]. Additionally, far-infrared absorption coefficients, α, covering 1.2–4.3 THz (40—144 cm^{-1}), were taken from Vij et al. [5] and converted to $\hat{\varepsilon}(\nu)$ with the help of the Kramers–Kronig (KK) relation [25]

$$n(\bar{\nu}_i) - n_\infty = \frac{1}{2\pi^2} \int_0^\infty \frac{\alpha(\bar{\nu})}{\bar{\nu}^2 - \bar{\nu}_i^2} \, \mathrm{d}\bar{\nu} \tag{1}$$

and the equations

$$\varepsilon' = n^2 - \left(\frac{\alpha}{4\pi\bar{\nu}}\right)^2 \tag{2}$$

$$\varepsilon'' = \frac{n\alpha}{2\pi\bar{\nu}} \tag{3}$$

relating the refractive index, $n(\bar{\nu})$, and the absorption coefficient, $\alpha(\bar{\nu})$, at wavenumber $\bar{\nu} = \nu/c_0$ to the corresponding permittivity, $\varepsilon'(\bar{\nu})$, and loss, $\varepsilon''(\bar{\nu})$; c_0 is the speed of light in vacuo [26].

For the KK transformation the data for $\varepsilon'(\bar{\nu})$ and $\varepsilon''(\bar{\nu})$ determined in our laboratory were first converted into $n(\bar{\nu})$ and $\alpha(\bar{\nu})$. The resulting absorption coefficients were combined with the $\alpha(\bar{\nu})$ values extracted from the digitized far-infrared spectrum of Ref. [5] at 298 K (their Fig. 1). To match both sets of data in the overlapping region of 1.2–2.3 THz (40—77 cm^{-1}) the $\alpha(\bar{\nu})$ values from the literature had to be multiplied by 1.1. This might be due to errors in the digitization of the graph, as well as due to inaccuracies of the far-infrared spectra themselves (no instrument details, like optical path length, were given). The refractive index was then calculated for the region $1.2 \leqslant \nu/\mathrm{THz} \leqslant 4.3$ (40—144 cm^{-1}) by numerical integration of Eq. (1) with the trapezoidal method. The anchor value for the refractive index, n_∞, was adjusted for best overlap of experimental and calculated $n(\bar{\nu})$ in 1.2–2.3 THz (40—77 cm^{-1}). The obtained $\hat{\varepsilon}(\nu)$ spectrum is displayed in Fig. 3; Fig. 4 shows the corresponding spectra of refractive index and absorption coefficient.

For the formal description of $\hat{\varepsilon}(\nu)$ various relaxation models based on sums of up to four individual contributions to the spectrum were tested with a non-linear least-squares routine which simultaneously fits $\varepsilon'(\nu)$ and $\varepsilon''(\nu)$ [27,28]. The quality of the fit was evaluated by the reduced error function χ^2_r

$$\chi^2_\mathrm{r} = \frac{1}{2N - m - 1} \left[\sum_{i=1}^{N} w_{\varepsilon'}(\nu_i) \delta\varepsilon'(\nu_i)^2 + \sum_{i=1}^{N} w_{\varepsilon''}(\nu_i) \delta\varepsilon''(\nu_i)^2 \right] \tag{4}$$

where $\delta\varepsilon'(\nu_i)$ and $\delta\varepsilon''(\nu_i)$ are the residuals, N is the number of data triples $(\nu_i, \varepsilon'(\nu_i), \varepsilon''(\nu_i))$, and m the number of the adjustable parameters. Experimental data were weighted statistically ($w_{\varepsilon''}(\nu_i) = |\varepsilon''(\nu_i)^{-1}|$ and $w_{\varepsilon'}(\nu_i) = |\varepsilon'(\nu_i)^{-1}|$) to give the values of ε' and ε'' equal importance in the simultaneous fit with Eqs. (5) and (6).

3. Results and discussion

3.1. Dichloromethane at 25 °C

In accordance with previous literature [8,9], at high frequencies, $\nu > 100$ GHz, the dielectric spectra of DCM (Figs. 2 and 3) deviate considerably from the shape expected for simple exponential relaxation, indicating the onset of molecular librations. Evaluation of the various fit models tested for the 25 °C spectra (Fig. 3) indeed revealed the presence of three modes: the main dispersion step centered at ~70 GHz and two high-frequency modes peaking at ~0.4 THz and ~1.8 THz in the $\hat{\varepsilon}(\nu)$ representation (corresponding to the shoulder at ~0.9 THz (~30 cm^{-1}) and the peak at ~2.3 THz (~77 cm^{-1}) in $\alpha(\nu)$, Fig. 4).

Two libration modes could be expected from the symmetry of CH_2Cl_2. Therefore, the high-frequency contributions were both modeled as damped harmonic oscillators (DHOs) with resonance frequencies, ν_i ($i = 2, 3$), and damping constants, γ_i. For the feature at ~70 GHz associated with DCM relaxation a symmetrically broadened Cole–Cole equation was suggested [8], albeit with a very small width parameter of $\alpha_\mathrm{CC} = 0.03$. For the present spectra a Debye equation (D, $\alpha_\mathrm{CC} \doteq 0$) is sufficient to model $\hat{\varepsilon}(\nu)$ at low frequencies. However, correction for the inertial rise of dipole reorientation is required to avoid unphysical far-infrared contributions of the Debye equation in the D + DHO + DHO description of the spectrum [29], see Fig. 4. We therefore use the modified Debye equation (D$^\mathrm{i}$) suggested by Turton and Wynne [30], which contains the inertial rise constant, γ_lib, in addition to the dielectric relaxation time, τ_1, yielding the D$^\mathrm{i}$ + DHO + DHO model

$$\hat{\varepsilon}(\nu) = \frac{\varepsilon - \varepsilon_2}{1 - (1 + \gamma_\mathrm{lib}\tau_1)^{-1}} \cdot \left(\frac{1}{1 + (\mathrm{i}2\pi\nu\tau_1)} - \frac{1}{1 + \mathrm{i}2\pi\nu\tau_1 + \gamma_\mathrm{lib}\tau_1} \right) + \frac{(\varepsilon_2 - \varepsilon_3)\nu_2^2}{\nu_2^2 - \nu^2 + \mathrm{i}\nu\gamma_2} + \frac{(\varepsilon_3 - \varepsilon_\infty)\nu_3^2}{\nu_3^2 - \nu^2 + \mathrm{i}\nu\gamma_3} + \varepsilon_\infty \tag{5}$$

In Eq. (5) the static relative permittivity ε, as well as ε_2, ε_3, and ε_∞ are the limits of the individual dispersion steps to $\varepsilon'(\nu)$ which define the amplitudes $S_1 = \varepsilon - \varepsilon_2$, $S_2 = \varepsilon_2 - \varepsilon_3$, and $S_3 = \varepsilon_3 - \varepsilon_\infty$ of the three modes. According to Turton and Wynne [30] the inertial rise constant, γ_lib, is in the order of the average librational frequency and thus associated with the resonance frequencies of the two DHO modes of Eq. (5). Trial fits, where γ_lib was varied in the range of 1.5–2.5 THz, revealed a small but not systematic effect on χ^2_r

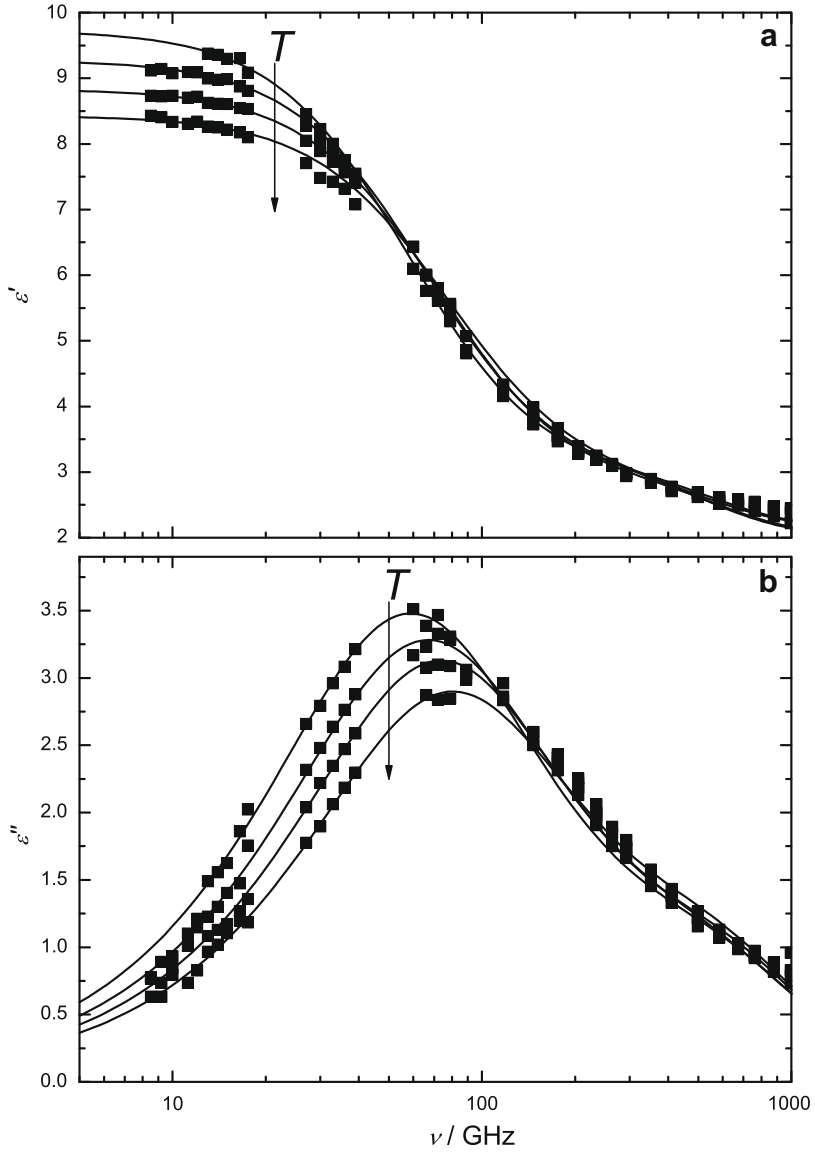

Fig. 2. (a) Dielectric permittivity, ε', and (b) dielectric loss, ε'', of dichloromethane at temperatures from 278.15 to 308.15 K. Symbols show experimental data, lines represent the D^i + DHO fit. Arrows indicate increasing temperature.

and negligible cross-correlations of this quantity with the remaining fit parameters. Thus, we fixed the inertial rise constant to $\gamma_{lib} = 2$ THz in the final fit presented in Table 1. As can be seen from Figs. 3 and 4 this D^i + DHO + DHO model provides a very good fit of the experimental spectrum at 25 °C, albeit with a small low-frequency shift for the calculated maximum ($\sim$71 cm^{-1}) of the absorption coefficient, α, relative to the experimental value ($\sim$77 cm^{-1}; Fig. 4).

As shown below, the relaxation centred $\sim$70 GHz, which dominates the dielectric spectrum, $\hat{\varepsilon}(\nu)$ (Fig. 3), can be unambiguously assigned to the rotational diffusion of CH_2Cl_2 dipoles. The two DHO modes resonating at $\sim$30 cm^{-1} (0.893 THz) and $\sim$71 cm^{-1} (2.13 THz) determine the shoulder and the peak observed for $\alpha(\nu)$ (Fig. 4). The ratio of the resonance frequencies, $\nu_3/\nu_2 \approx 2.4$, compares well with the ratio of libration frequencies expected from the moments of inertia perpendicular to the dipole vector, $\sqrt{I_y/I_x} \approx 3$ [8]. In accordance with the simulations of Isegawa and Kato [14] this suggests that the far-infrared spectrum of DCM is dominated by librations of the permanent dipoles. However, the simulations also reveal that further spectral contributions, arising from induced moments and especially cross-correlations, are far from negligible. Neglect of these broad bands in our fit model, Eq. (5), may explain the deviations between experimental and calculated spectrum around 70 cm^{-1} (Fig. 4). However, due to the limited accuracy of the digitized literature data [5] forming our experimental basis above 50 cm^{-1} implementation of a more elaborate fit model appeared not to be expedient.

3.2. Temperature dependence

Based on the above results, we now want to discuss the temperature dependence of DCM relaxation. Unfortunately, the spectral range of the THz-TDS in the transmission setup was limited to $\lesssim$ 1 THz due to the high absorption of DCM so that the low-frequency libration (ν_2 mode of Eq. (5)) is covered up to its resonance frequency ν_2, whereas only the onset of the ν_3 libration is in the experimental frequency window. Unfortunately, the latter contribution, which cannot be neglected at

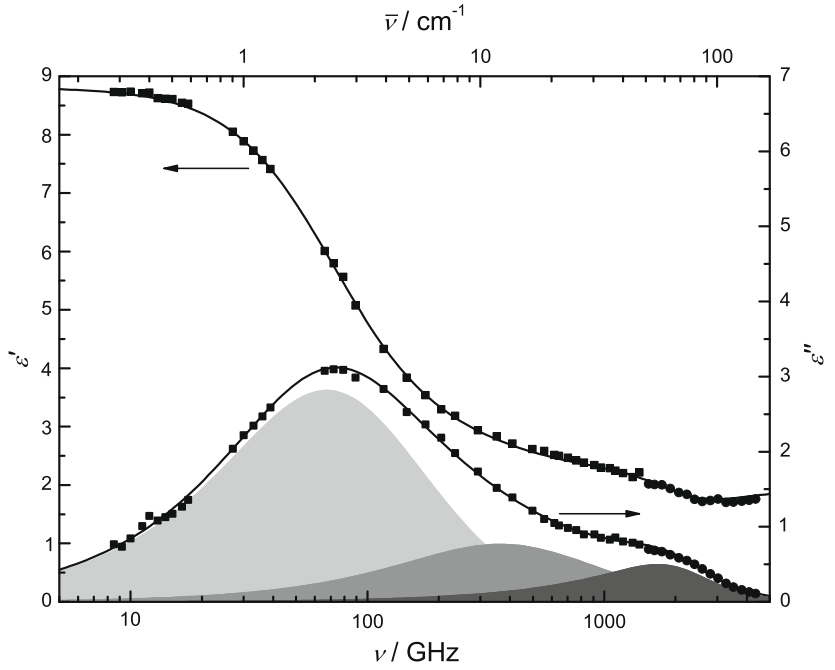

Fig. 3. Dielectric permittivity, ε', and loss, ε'', of dichloromethane at 25 °C: ■ experimental data of this work; ● values obtained by Kramers–Kronig transformation of literature data [5]. Lines represent fit with the $D^i + DHO + DHO$ model, shaded areas indicate the contributions of the modified Debye (D^i) and the two DHO modes.

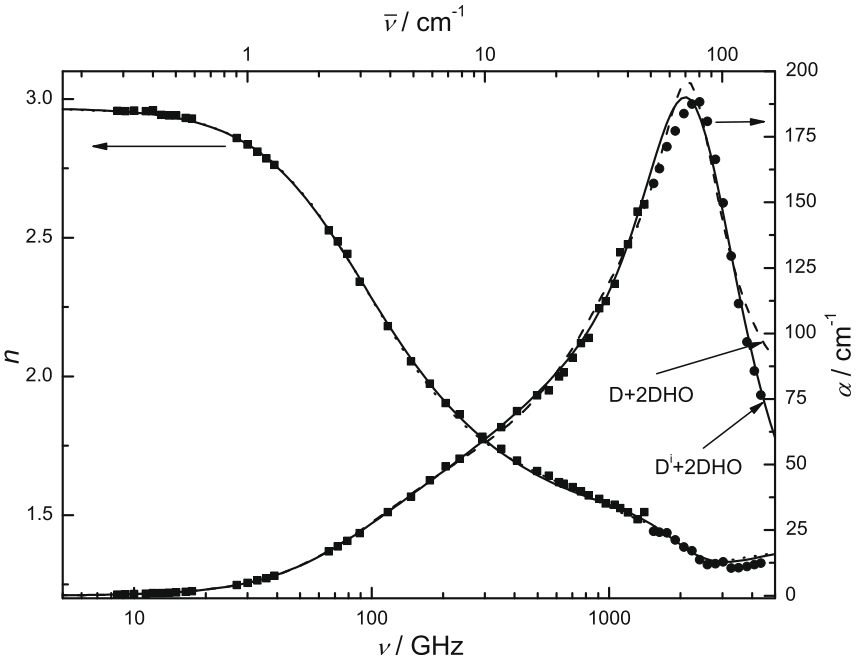

Fig. 4. Refractive index, n, and absorption coefficient, α, of dichloromethane at 25 °C: ■ experimental data of this work; ● values obtained by Kramers–Kronig transformation of literature data [5]. Solid lines represent fit with the modified $D^i + DHO + DHO$ model, dashed lines the fit with the classical D + DHO + DHO model.

Table 1
Parameters (limiting permittivities, ε_j, relaxation time, τ_1, inertial rise constant, γ_{lib}, damping constants, γ_j, resonance frequencies, ν_j, and reduced error function, χ_r^2) of the $D^i + DHO + DHO$ model, Eq. (5), fitting $\hat{\varepsilon}(\nu)$ of dichloromethane at 25 °C in the frequency range $8.5 \leqslant \nu/\text{GHz} \leqslant 4300$.

ε	τ_1 (ps)	γ_{lib} (THz)	ε_2	γ_2 (THz)	ν_2 (THz)	ε_3	γ_3 (THz)	ν_3 (THz)	ε_∞
8.81	2.23	2[a]	3.89	2.44	0.893	2.56	2.79	2.13	1.98

[a] Parameter fixed during fitting procedure. $\chi_r^2 = 96.4 \times 10^{-5}$.

$\sim$ 1 THz (see Fig. 3), is too far outside the spectral range covered in the experiment to be properly resolved in the fit. Consequently, its presence slightly biases the fits of the temperature-dependent spectra.

Table 2
Parameters (limiting permittivities, ε_j, relaxation time, τ_1, inertial rise constant, γ_{lib}, damping constant, γ_2, resonance frequency, ν_2, and reduced error function, χ^2_r) of the $D^i + DHO$ model at the investigated temperatures, T.

T (K)	ε	τ_1 (ps)	γ_{lib} (THz)	ε_2	γ_2 (THz)	ν_2 (THz)	ε_3	$\chi^2_r \times 10^5$
278.15	9.73	2.74	2[a]	3.91	1.88	0.89[a]	2.44	228
288.15	9.27	2.41	2[a]	3.92	1.94	0.89[a]	2.43	242
298.15	8.83	2.17	2[a]	3.77	1.76	0.89[a]	2.36	188
308.15	8.43	2.03	2[a]	3.88	1.86	0.89[a]	2.34	369

[a] Parameter fixed during fit procedure.

Different models have been tested to describe the experimental data of Fig. 2. It was found that the best fit was achieved with the $D^i + DHO$ model

$$\hat{\varepsilon}(\nu) = \frac{\varepsilon - \varepsilon_2}{1-(1+\gamma_{lib}\tau_1)^{-1}} \cdot \left(\frac{1}{1+(i2\pi\nu\tau_1)} - \frac{1}{1+i2\pi\nu\tau_1+\gamma_{lib}\tau_1} \right) + \frac{(\varepsilon_2-\varepsilon_3)\nu_2^2}{\nu_2^2-\nu^2+i\nu\gamma_2} + \varepsilon_3 \quad (6)$$

where the resonance frequency of the DHO mode was fixed to the value obtained at 25 °C, $\nu_2 = 0.89$ THz. This procedure seems reasonable as in contrast to relaxation processes the location of libration modes depends only weakly on temperature [5].

The obtained parameters are listed in Table 2, Fig. 2 compares fits and experimental data. The small deviations at $\nu \gtrsim 100$ GHz can almost certainly be attributed to the small contribution of the neglected 2 THz resonance (Fig. 3). Nevertheless, comparison of the 298 K data from Table 2 with results of the full fit (Table 1) reveals that the dielectric parameters ε, ε_2, ε_3, and τ_1 obtained with the $D^i + DHO$ model are only weakly biased by the limitation of the spectral range to $\leqslant 1$ THz (Fig. 5). At all temperatures the extrapolated static permittivities, ε, of this study are in excellent agreement with data obtained with conventional capacitor methods [1]. Additionally, the value of ε_∞ obtained with the $D^i + DHO + DHO$ model at 25 °C (Table 1 and Fig. 5) and the squared refractive index of Ref. [31] agree within our experimental uncertainty, suggesting that the full intermolecular dynamics of DCM is practically covered at 25 °C. On the other hand, the static permittivity and the relaxation time obtained by Vij et al. [8] from fitting a single Cole–Cole equation to their spectra deviate considerably from our results (Fig. 5). The same is true for the simulated ε and τ of Isegawa and Kato [14], probably reflecting the well-known difficulties encountered in the quantitative computer simulation of liquid-state dielectric properties [32].

Comparison of τ_1 with relaxation times from other experimental techniques allows to conclude on the mechanism behind the observed dielectric relaxation. For rotational diffusion of a molecule it is expected [11] that the molecular correlation times τ^L of rank L fulfill the relation

$$\tau^L = \frac{2\tau_{rot}}{L(L+1)} \quad (7)$$

where τ_{rot} ($= \tau^{L=1}$) is the rotational correlation time of a probed intramolecular vector. Correlation times accessible with NMR and Raman spectroscopy are single-particle relaxation times of rank $L = 2$. Dielectric spectroscopy probes $L = 1$ but the experimentally accessible relaxation time (τ_1 of Table 2) is a collective property [11] which has to be converted to the corresponding rotational correlation time with the Powles–Glarum equation [33,34]

$$\tau_{rot} = \frac{2\varepsilon + \varepsilon_\infty}{3\varepsilon}\tau_1 \quad (8)$$

The obtained values for τ_{rot} are displayed in Fig. 6.

For isotropic rotational diffusion τ_{rot} is independent of the chosen vector, whereas in the case of anisotropic reorientation CH_2Cl_2 rotation around the x-axis (Fig. 1) should be different from that around the y- and z-axes [15]. Thus τ_{rot} should depend on the orientation of the monitored vector relative to (x,y,z), with DS only monitoring rotations around x and y. If the moments of inertia, $I_x \ll I_y \approx I_z$, were determining DCM dynamics, then $\sqrt{10}\tau_x \approx \tau_y \approx \tau_z$ would be expected. The difference between reorientation around x and the other axes should be less pronounced (of the order of $1.5\tau_x \approx \tau_y \approx \tau_z$) if viscous friction combined with the asymmetry in the molecular shape predominates [15].

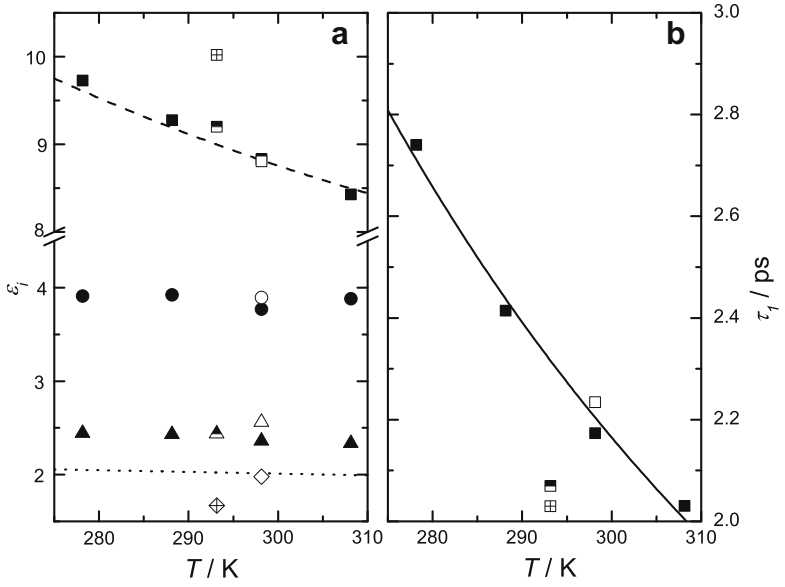

Fig. 5. (a) Limiting permittivities (ε: squares, ε_2: circles, ε_3: triangles, and ε_∞: diamonds) extracted from DCM spectra with Eqs. (5) and (6), together with the squared refractive index, $n^2_{633\ nm}$ ([31], dotted line) and the static permittivity, ε (dashed line), determined with low-frequency capacitance measurements [1]. (b) Relaxation time τ_1 (symbols) and fit with Eq. (10) (line). Open symbols represent parameters obtained at 25 °C with the $D^i + DHO + DHO$ model from the spectrum covering 8.5 GHz $\leqslant \nu \leqslant$ 4.3 THz; filled symbols show the results of the $D^i + DHO$ model applied to the restricted frequency range of 8.5 GHz $\leqslant \nu \lesssim$ 1 THz. Also included are literature data from Vij et al. [8] (half filled symbols) and from Isegawa and Kato [14] (open symbols with cross).

Intuitively, one would expect the latter situation for the diffusive reorientation of a molecule in a dense medium. However, based on the comparison of ^{13}C- and ^{35}Cl NMR data Rodriguez et al. [15] concluded that DCM reorientation is highly anisotropic and determined by inertial motion. This may be a reflection of different weights of both librational motions of DCM on the time-integrated relaxation times determined by ^{13}C- and ^{35}Cl NMR. On the other hand, it should be noted that the value of τ_{rot} from ^{35}Cl NMR is rather sensitive to the choice of the quadrupole coupling constant required for the analysis of the experimental relaxation rates. Hacura et al. [16] determined the rotational correlation times of the vectors associated with three Raman bands as a function of temperature and pressure. According to this study, and in contrast to the above NMR results, the observed correlation times for rotation around *x*, *y*, and *z* do not differ within experimental accuracy at those temperatures relevant to the present study, suggesting rather isotropic reorientation. The situation becomes even less clear when the widely scattering correlation times compiled in Ref. [7] are also considered.

Fig. 6 compares the τ_{rot} data determined in this investigation with rotational correlation times from ^{13}C NMR studies [15] and averaged τ_{rot} values calculated from the Raman data of Hacura et al. [16]. Clearly, the agreement between the different techniques is very good. Since none of the vectors probed by NMR and Raman coincides with the dipole vector it can be concluded that DCM reorientation is isotropic in the diffusive regime. This is in line with the observation that a Debye equation is sufficient to describe the low-frequency component of $\hat{\varepsilon}(\nu)$.

Analysis of the temperature dependence of τ_{rot} in terms of the extended Stokes–Einstein–Debye theory (SED) [35]

$$\tau_{rot} = \frac{3V_{eff}\eta}{k_B T} + \tau^0_{rot} \tag{9}$$

yields the effective volume of rotation, V_{eff}, required by a CH_2Cl_2 molecule. In Eq. (9) k_B is the Boltzmann constant and T the thermodynamic temperature. $V_{eff} = fCV_m$, is determined by the molecular volume, V_m, and the shape factor, f, of the particle [36]. Additionally, a hydrodynamic friction coefficient, C, appears which is generally treated as an empirical parameter but its limiting values for *stick* ($C_{stick} = 1$) and *slip* ($C_{slip} = 1 - f^{-2/3}$) boundary conditions are known. The empirical axis intercept, τ^0_{rot}, is occasionally interpreted as the correlation time of the freely rotating particle.

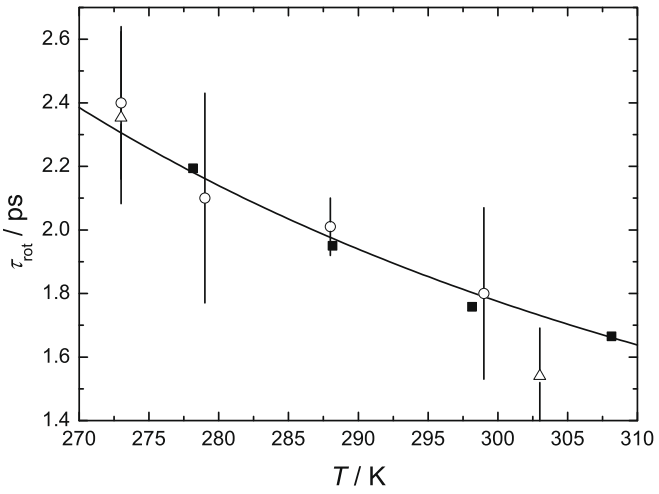

Fig. 6. Rotational correlation times, τ_{rot}, from dielectric spectroscopy (■, this study), ^{13}C NMR (○, Ref. [15]) and Raman spectroscopy (△, Ref. [16]). Line represents the fit of the DS data with Eq. (9).

The viscosities, η, required for the SED analysis of the rotational correlation times of this investigation were taken from the literature [1]. Assuming *slip* boundary conditions ($C_{slip} = 0.129$) a weighted fit of τ_{rot} *vs.* $1/T$ yields the molecular volume of $V_m = (25 \pm 1)$ Å^3 from the slope, whereas 59 Å^3 was estimated by approximating the DCM molecule as a prolate ellipsoid with principal axes of lengths $a = 6.52$ Å and $b = c = 4.16$ Å ($f = 1.230$; from van der Waals radii [37] of the atoms). This difference, yielding $C = 0.06$, may point at *sub-slip* friction for DCM reorientation. However, it should be kept in mind that a prolate ellipsoid is certainly only a rough approximation for CH_2Cl_2. Similar caution applies for the obtained axis intercept, $\tau^0_{rot} = (0.59 \pm 0.01)$ ps. Although comparable to the free-rotor correlation time [38] for rotation around the *y*-axis (0.3 ps) discussion of this quantity is not appropriate.

Further insight into the mechanism of DCM relaxation is provided by its Eyring [39] activation enthalpy, $\Delta H^{\neq}$, and entropy, $\Delta S^{\neq}$, which can be derived from the temperature dependence of τ_1

$$\ln(T\tau_1) = \left[\ln\left(\frac{h}{k_B}\right) - \frac{\Delta S^{\neq}}{R}\right] + \frac{\Delta H^{\neq}}{RT} \tag{10}$$

In Eq. (10) h and R are the Planck and the gas constant, respectively. From the τ_1 data of Table 2 the activation enthalpy of $\Delta H^{\neq} = (4.8 \pm 0.5)$ kJ mol^{-1} and the activation entropy of $\Delta S^{\neq} = (-5.8 \pm 1.8)$ J K^{-1} mol^{-1} were obtained (Fig. 5b). These values are comparable to the activation parameters of acetonitrile ($\Delta H^{\neq} = (4.6 \pm 0.2)$ kJ mol^{-1}; $\Delta S^{\neq} = (-9.8 \pm 0.6)$ J K^{-1} mol^{-1} [40]), which is also regarded as a simple dipolar liquid. The significantly smaller value of $|\Delta S^{\neq}|$ for DCM suggests that compared to acetonitrile smaller structural changes of the environment are required for the reorientation of a CH_2Cl_2 molecule, meaning that DCM dynamics are less cooperative.

Under the assumption that the fast dipole moment fluctuations associated with the librations do not correlate with the slower rotational diffusion, the effective dipole moment, μ_{eff}, of the DCM molecules in the liquid can be obtained from the relaxation amplitude, S_1, with the Cavell equation [41]

$$\frac{2\varepsilon + 1}{\varepsilon} \cdot S_1 = \frac{N_A c}{k_B T \varepsilon_0} \cdot \mu^2_{eff} \tag{11}$$

where N_A is the Avogadro constant, ε_0 the vacuum permittivity and c is the molar concentration of DCM, calculated from the density data of Ref. [1]. Averaging over all investigated temperatures the data of Table 2 yield the effective dipole moment of $\mu_{eff} = (1.93 \pm 0.04)$ D for CH_2Cl_2.

μ_{eff} relates to the dipole moment of the isolated molecule, μ, via

$$\mu_{eff} = \sqrt{g}\mu_{ap} = \frac{\sqrt{g}\mu}{1 - f_r\alpha} \tag{12}$$

where $\alpha = 6.82$ Å^3 [3] is the molecular polarizability and f_r the reaction field factor [42] of DCM. The Kirkwood factor $g = \mu^2_{eff}/\mu^2_{ap}$ is a measure for orientational correlations among the dipoles in the liquid [42].

Under the assumption of a spherical reaction field of radius $a/2 = 3.26$ Å for DCM insertion of $\mu = 1.61$ D [3] into Eq. (12) yields the value of $\mu_{ap} = 1.93$ D, thus $g = 1$. The virtual identity of the experimental μ_{eff} and the calculated μ_{ap} is certainly accidental.[1] Nevertheless, this finding indicates negligible orientational correlations among neighboring dipoles, a result which is in line with the inference from τ_1 that DCM relaxation can be viewed as essentially isotropic rotational diffusion of individual dipoles. This is also supported by a comparison of g with the Kirkwood correlation

[1] Insertion of $(\varepsilon - \varepsilon_\infty)$ instead of S_1, *i.e.* assumption that dipole fluctuations associated with librations and rotational diffusion are correlated, yields $g \approx 1.3$.

factors given by Richardi et al. [43]: $g_K = 1.07$ from experimental static permittivity data and $g_K = 1.15$ calculated with statistical mechanics (note the slightly different assumptions behind the Kirkwood–Fröhlich [42] and the Cavell [41] equations).

4. Conclusions

The dielectric properties of dichloromethane over a wide frequency range have been investigated. Data analysis reveals three contributions to $\hat{\varepsilon}(\nu)$, a relaxation at ~ 70 GHz modeled by a modified Debye equation accounting for inertial rise, and two fast modes at ~ 0.4 THz and ~ 1.8 THz described by damped harmonic oscillators with resonance frequencies of $\nu_2 = 0.89$ THz and $\nu_3 = 2.1$ THz. The relaxation at low frequencies can be assigned to rotational diffusion of the dipolar DCM molecules. The data suggest that the diffusive reorientation of the dipole vectors is isotropic. There are no indications for orientational correlations among the CH_2Cl_2 molecules. The two fast modes in the THz region are dominated by the libration of the permanent CH_2Cl_2 dipoles around the *x*- and *y*-axes of the molecule (Fig. 1), albeit some contributions from induced moments and dipole-induced dipole cross-correlations are likely.

Acknowledgements

The authors thank Prof. W. Kunz (Regensburg) and Prof. H. Helm (Freiburg) for the provision of laboratory facilities and Dr. D.A. Turton and Prof. K. Wynne for helpful discussion about fitting models.

References

[1] D.R. Lide (Ed.), CRC-Handbook of Chemistry and Physics, 85th edn., CRC-Press, Boca Raton, 2004.
[2] S.S. Chadwick, Ullmann's Encyclopedia of Industrial Chemistry, Wiley–VCH, Weinheim, 2006.
[3] M.W. Evans, G.J. Evans, W.T. Coffey, P. Grigolini, Molecular Dynamics, Wiley, New York, 1982.
[4] M.W. Evans, J. Yarwood, Adv. Mol. Relax. Interact. Process. 21 (1981) 1.
[5] J.K. Vij, C.J. Reid, G.J. Evans, M. Ferrario, M.W. Evans, Adv. Mol. Relax. Interact. Process. 22 (1982) 79.
[6] J.K. Vij, Y.P. Kalmykov, J. Chem. Phys. 99 (1993) 2506.
[7] M.W. Evans, M. Ferrario, Adv. Mol. Relax. Interact. Process. 23 (1982) 113.
[8] J.K. Vij, F. Hufnagel, T. Grochulski, J. Mol. Liq. 49 (1991) 1.
[9] Z. Kisiel, K. Leibler, A. Gerschel, J. Phys. E: Instrum. 17 (1984) 240.
[10] D. Bertolini, M. Cassettari, G. Salvetti, T.E.S. Veronesi, Rev. Sci. Instrum. 12 (1990) 61.
[11] C.F.J. Böttcher, P. Bordewijk, Theory of Electric Polarization, vol. 2, Elsevier, Amsterdam, 1978.
[12] F. Kremer, A. Schönhals (Eds.), Broadband Dielectric Spectroscopy, Springer, Berlin, 2003.
[13] H. Torii, J. Mol. Liq. 119 (2005) 31.
[14] M. Isegawa, S. Kato, J. Chem. Phys. 127 (2007) 244502.
[15] A.A. Rodriguez, S.J.H. Chen, M. Schwartz, J. Magn. Reson. 74 (1987) 114.
[16] A. Hacura, T.W. Zerda, M. Kaczmarski, J. Raman Spectrosc. 11 (1981) 427.
[17] B. Gestblom, I. Svorstøl, J. Songstad, J. Phys. Chem. 90 (1986) 4684.
[18] V.P. Pawar, S.C. Mehrotra, J. Mol. Liq. 108 (2003) 95.
[19] S. Schrödle, G. Annat, D.R. MacFarlane, M. Forsyth, R. Buchner, G. Hefter, Chem. Commun. (2006) 1748.
[20] J. Hunger, A. Stoppa, R. Buchner, G. Hefter, J. Phys. Chem. B 112 (2008) 12913.
[21] S. Schrödle, R. Buchner, W. Kunz, J. Phys. Chem. B 108 (2004) 6281.
[22] J. Barthel, K. Bachhuber, R. Buchner, H. Hetzenauer, M. Kleebauer, Ber. Bunsen-Ges. Phys. Chem. 95 (1991) 853.
[23] P. Uhd Jepsen, B.M. Fischer, A. Thoman, H. Helm, J.Y. Suh, R. Lopez, R.F. Haglund, Phys. Rev. B 74 (2006) 205103.
[24] B.M. Fischer, Ph.D. Dissertation, Freiburg, Germany, 2005.
[25] J.E. Bertie, S.L. Zhang, C.D. Keefe, Vib. Spectr. 8 (1995) 215.
[26] J.R. Birch, T.J. Parker, in: K.J. Button (Ed.), Infrared and Millimeter Waves, vol. 2, Academic Press, New York, 1979.
[27] R. Buchner, T. Chen, G. Hefter, J. Phys. Chem. B 108 (2004) 2365.
[28] A. Stoppa, J. Hunger, R. Buchner, G. Hefter, A. Thoman, H. Helm, J. Phys. Chem. B 112 (2008) 4854.
[29] S. Havriliak, S.J. Havriliak, Dielectric and Mechanical Relaxation in Materials, Hanser, New York, 1997.
[30] D.A. Turton, K. Wynne, J. Chem. Phys. 128 (2008) 154516.
[31] S. Valkai, J. Liszi, I. Szalai, J. Chem. Thermodynam. 30 (1998) 825.
[32] C. Schröder, J. Hunger, A. Stoppa, R. Buchner, O. Steinhauser, J. Chem. Phys. 129 (2008) 184501.
[33] J.G. Powles, J. Chem. Phys. 21 (1953) 633.
[34] S.H. Glarum, J. Chem. Phys. 33 (1960) 639.
[35] J.C. Dote, D. Kivelson, R.N. Schwartz, J. Chem. Phys. 85 (1981) 2169.
[36] J.C. Dote, D. Kivelson, J. Phys. Chem. 87 (1983) 3889.
[37] K. Tanabe, Spectrochim. Acta 32 (1976) 1129.
[38] F.J. Bartoli, T.A. Litovitz, J. Chem. Phys. 56 (1972) 413.
[39] S. Glasstone, K.J. Laidler, H. Eyring, The Theory of Rate Processes, McGraw-Hill, New York, 1941.
[40] A. Stoppa, S. Schrödle, G. Hefter, R. Buchner, unpublished results.
[41] E.A.S. Cavell, P.C. Knight, M.A. Sheikh, Trans. Faraday Soc. 67 (1971) 2225.
[42] C.F.J. Böttcher, Theory of Electric Polarization, vol. 1, Elsevier, Amsterdam, 1973.
[43] J. Richardi, P.H. Fries, H. Krienke, J. Phys. Chem. B 102 (1998) 5196.